AD-A081 983 TEXAS UNIV AT AUSTIN DEPT OF PHYSICS F/G 20/9
FORMATION & DIAGNOSTICS OF A CYLINDRICAL SHELL PLASMA,(U)
1980 R D BENGTSON, D L HONEA, D PEASE $AFOSR-77-3259
UNCLASSIFIED AFOSR-TR-80-0172 NL

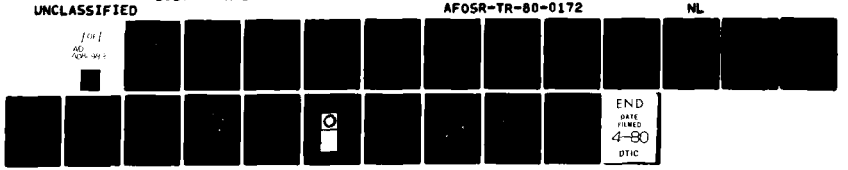

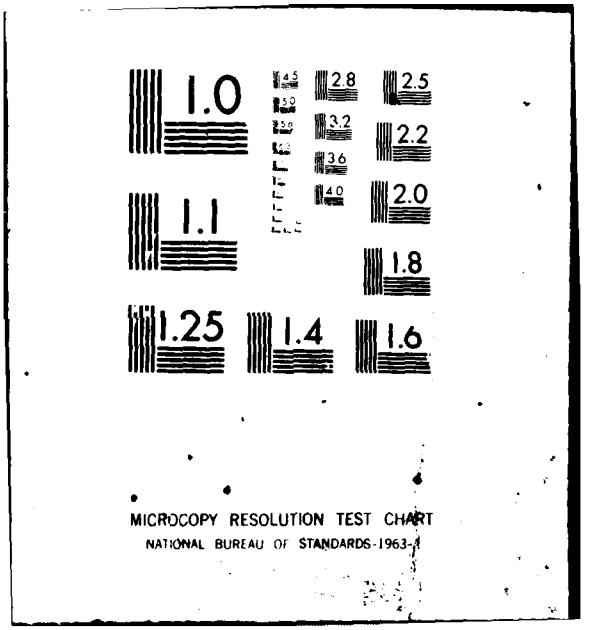
1.0
1.1
1.25
1.4
1.6
1.8
2.0
2.2
2.5
2.8
3.2
3.6
4.0
MICROCOPY RESOLUTION TEST CHART
NATIONAL BUREAU OF STANDARDS-1963-A

FINAL TECHNICAL REPORT

Formation & Diagnostics of a Cylindrical Shell Plasma

Air Force Office of Sponsored Research

LEVEL II

by

Roger D. Bengtson D. L. Hanna D. Pen...
Department of Physics
The University of Texas
Austin, Texas 78712

Report # AFOSR-77-3259

PRODUCTION OF A CYLINDRICAL PLASMA SHELL

by

Roger D. Bengtson, D.L. Honea and D. Pease
Department of Physics
University of Texas at Austin
Austin, Texas 78712

and

James H. Degnan and Robert A. Golobic[++]
Air Force Weapons Laboratory
Kirtland AFB, Albuquerque, New Mexico

and

ABSTRACT

An apparatus was developed which forms a hollow cylindrical plasma shell of 3 x 2 cm^2 cross section 40 cm diameter by injecting a neutral gas shell of argon via supersonic injection nozzles and ionizing this shell with a high voltage electrical discharge.

[++]Consultant. Present address: Centennial Sciences, Colorado Springs, Colorado 80907

I. Introduction

Various aspects of obtaining high temperature, high density plasmas from imploding cylindrical liners have been considered by Turchi and Baker.[1] Their method is essentially a hollow Z pinch geometry where the collapse is driven by the J x B force produced by the discharge current magnetic field. Implementation of these concepts and the results obtained have been reported by Baker, et al.,[2] and Burns, et al.[3] in articles describing X-ray spectroscopic data from high energy implosions of aluminum and aluminized plastic liners.

As an alternate approach to metal foils, the use of gas shells as the implosion mass offer several possible advantages. The wider range of atomic number available in gas shells allows the use of smaller implosion mass and thus much higher implosion energy per unit mass for a given energy storage facility. The greater range in choice of atomic mass number allows optimization of transfer of stored energy to implosion energy by load matching. From a purely operational standpoint, the use of gas puffs gives the ability for repeated firing of the apparatus without entering the vacuum.

Optimization of power multiplication in the implosion phase requires that the initial plasma shell be cylindrically symmetric, have a high degree of ionization and a reasonable thickness. Using a gas puff to establish a neutral gas shell with the desired homogeneity which is then ionized, one is more assured of having a uniformly ionized plasma shell with high repeatability. Thus by separating the creation of the initial plasma shell from the application of the fast, high energy implosion pulse it may be easier to manipulate the crucial initial conditions.

In addressing these requirements we have developed and operated a supersonic flow through gas injection and ionization system to produce an ionized implosion load in the form af a 20 cm radius, 2 cm tall, 3 cm thick cylindrical gas shell plasma. The most similar related work is that on small radius (1-2 cm) cylindrical gas shell formation and hollow Z-pinch work done at University of California, Irvine (Shilo, et al.)[4] and Physics International (Stallings, et al.).[5] In the following section we describe the gas injection system while Section III covers the ionization system and the diagnostics used to characterize it. Section IV summarizes the results and discusses further applications.

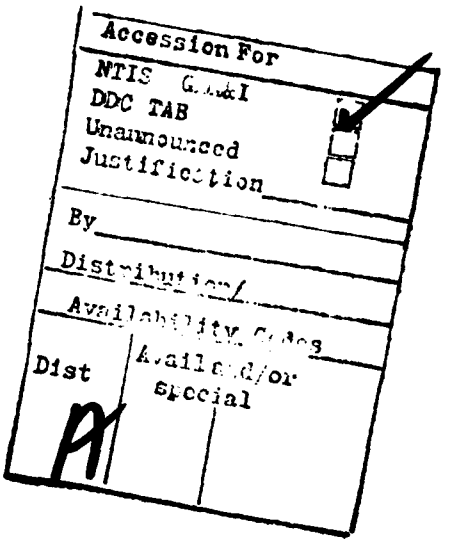

II. Gas Injection System

The basic consideration in the nozzle design was to provide a simple nozzle shape which could be easily fabricated. Conical nozzles in the lower electrode plate complemented by conical diffusers in the upper electrode were considered the best compromise. In addition the number of nozzles and their associated hole diameters are restricted to permit adequate current flow between them. The nozzle throat must be large enough to pass sufficient mass to produce adequate densities in the shell. The expansion ratio of the nozzle is also important since it is the exit Mach number of the nozzle which will determine the magnitude of the free expansion divergence. The diffuser diameter was chosen such that 98% of the mass will flow through. This also restricts the circumferential distribution of mass and results in 36 spokes rather than a uniform shell. The basic nozzle was then determined from inviscid conical source flow employing the method of characteristics with axially symmetric flow.

Essential geometrical features of the gas injection system are shown in the cross sectional view in Figure 1. Thirty-six injection nozzles are arranged symmetrically on a 20 cm radius circle in opposing electrode plates. The upper electrode plate is separated from the corresponding lower assembly by a polyethelene insulator which maintains a 2 cm separation of the electrodes. The lower assembly remains at system ground potential while the upper assembly rises to negative potential during the pulse discharge. Diagnostic access is available through one 10 cm diameter upper port and five 2 cm diameter radial ports each separated from the next by 45°.

The basic functional sequence of the flow through geometry has three parts: fast gas valve, gas spreader and injection flow through nozzles. The fast gas reservoir can be operated in the plenum pressure range of 100-1000 PsiA, which with the present nozzle design produces a mass loading of .1-1 mg argon in the electrode gap. Gas is distributed evenly to the injection nozzles via a secondary plenum gas spreader driven by the primary plenum. During flow through conditions, gas is dumped into the evacuated volume above the diffuser.

Turning to the details of the gas injection, we used a Henins-Marshall[6] type puff valve. High pressure gas is held in a 1.5 cm^3 plenum by compressing a lexan rod against the plenum orifice. The compressed gas is released in a few hundred microseconds[7] by destroying a small Permali rod which releases the energy stored in the lexan rod.

Gas exit slots in the head of the fast gas valve are aligned with the aperture of the gas spreader flow channel to allow unimpeded gas glow from primary plenum to nozzle jets. The flow channel is simply a cylindrical gap extending from the head of the valve to slightly beyond the jets. In this geometry the gas spreader-secondary plenum is evacuated prior to firing and has a volume of about 900 cm^3. Primary to secondary plenum pressure ratio is therefore $\approx$1 Psi.

Supersonic flow through is established in the electrode gap by the nozzle geometry illustrated in Figure 2. Also details of the gas spreader-secondary plenum in the vicinity of the nozzle jets can be seen. Fabrication of the nozzle geometry is executed in a two-inch aluminum plate which serves the dual function of injection nozzle system and discharge electrodes. Typical back-

ground pressures are maintained at 10^{-6} torr prior to firing.

A reliable trigger pulse was obtained from an electrode gap positioned in the gas spreader. The gap is a marine spark plug mounted flush with the spreader plate to minimize disturbance of the gas flow. When the pressure rises above ~1.5 torr the gap breaks down, giving an output timing pulse which is relatively insensitive to mechanical jitter from shattering the Permali or to the exact details of flow conditions of plenum emptying or expansion in the spreader. Degnan[7] has found that the timing jitter of the appearance of the gas in the discharge gap relative to the trigger pulse from the pressure trigger gap can be held to $\pm 10\mu$sec for pressure trigger voltage >3.0 KV.

The apparatus thus far described has the purpose of establishing a gas torus with a suitably sharp radial profile between appropriate electrode plates. Excessive outwash from the jets, in addition to degrading the radial profile, would ultimately cause flashover problems in the vicinity of the insulator as well. To evaluate the injection-capture efficiency of the nozzle system, a fast ion gauge was used to measure the time resolved cold gas density profile as a function of radial position. A standard 6AH6 pentode with the outer envelope removed is used as the fast ion gauge. The collection volume of the tube gives a spatial resolution of about 1 cm^3 and a time response of 30μsec risetime to a sharp density discontinuity in argon. The calibration of the ion gauge was performed using a Baratron gauge as the reference. Several tubes were compared in the calibration, with no appreciable difference in tube response found. In taking transient measurements, tube to tube response consistency was assumed.

Transient density measurements were performed with the tube collection volume placed in three positions. Of primary interest was the response observed at R = 20.0 cm which gives the timing for the flow through conditions. Positioning at R = 23.0 cm gives some indication of the flashover problem to be expected at the insulator.

With the tube positioned over the jet, (R = 20 cm) it can be seen that injection is well underway by 500μsec after the pressure trigger pulse. Quasi-steady injection has not matured until some 700-800μsec after the pressure trigger timing pulse. Some modulation effects are occasionally observed, presumably due to hydrodynamic sloshing in the secondary plenum. The slow pressure rise observed at the R = 33.0 cm position suggests that insulator flashover will not be a problem for at least several hundred microseconds after injection, well after the period of interest. A similar long time scale rise due to background pressure increase is also observed at R = 15.5 cm and R = 0.0 cm as well. The conclusion from these results is that the gas flow through is sharply defined and has high capture efficiency.

III. Ionization of the Gas Shell

For some implosion experiments, it may be desirable to fire the implosion pulse into a preionized load. We also wanted to reduce the modulation of 36 independent posts without severely degrading the radial profile. For these reasons, we drive a weak current across the electrode gap.

Primary circuit inductance is provided by a coil to give a ringing frequency of 250 KHz. Typical ionization process time scales suggest a range of risetimes of 1-10 μsec for the ionizing current. Discharge currents of the order 30-50 kA are observed for capacitor bank voltages from 5-7 kV.

To insure the uniformity of the breakdown we found it necessary to place trigger needles in each jet. The needles are suspended in the center of the upper diffuser jets and consist of a streamlined .5 mm needle protruding into the gap about 1 cm. A negative 15 kV pulse without about .1 μsec risetime and several microsecond duration drives a low energy oscillating discharge from the needle to the lower electrode. To maximize uniformity, the needles are switched by a single switch. The trigger needle pulse generator as well as the main ionization discharge is triggered simultaneously after a delay interval from the pressure trigger timing pulse.

Homogeneity was monitored by a time integrated open shutter photo of the discharge as shown in Figure 3 along with typical voltage traces. The open shutter photo was taken through the upper port by viewing a cone mirror centered on the lower electrode which was visible through the upper electrode cutout. The 36 radial streaks of brightest luminosity correspond to the 36 jet positions. Even with the trigger needle system operating, homogeneity was

sometimes nonuniform or irreproducible for bank voltages less than 5 kV. Homogeneity was also degraded if the sharp edges of the jets are not maintained.

Several diagnostics were applied to the plasma, once a qualitatively acceptable degree of homogeneity was established. A double Langmuir probe was used to alleviate the problem of high plasma potentials characteristic of linear discharges. The probe consisted of two 2 mil platinum wires separated by about 2 mm and positioned on the electrode gap midplane. Tip position could be radially scanned to map the density profile. Ion saturation current was driven by a 22 volt battery connected across the two tips. Isolation of the oscilloscope was provided by using an insulated current transformer to monitor the probe saturation current as a function of time. Only about .2 mm of the platinum wire tips contact the plasma, the remainder being encased in glass capillary tubing.

Probe results are summarized in Figure 4. Normalized electron density profiles taken from probe data at two times in the discharge show electron density as a function of radial position from near the jet centerline to 25 mm out. The peaks at $\Delta R = 7$ mm and $\Delta R = 16$ mm approximately correspond to the edges of the lower and upper jets respectively. The sharp jet edges appear to dominate emission in these vicinities. There is also a high localized density peak near the trigger needle for $r \leq 1.5$ mm.

Langmuir probe theory can not be reliably extended into the realm of the high density gradients to be expected in this situation. For this reason, absolute density measurements were taken with spectroscopic methods.

The Langmuir probes were used primarily to map the relative spatial dependence whereas the spectroscopic techniques provided an electron density and plasma temperature averaged over the optical collection volume. Time behavior of the electron density observed by the probes agrees well with the spectroscopic results of argon luminosity time behavior.

Both time resolved and wavelength resolved spectral emissions were observed from the plasmas by using two independent spectrometers. Line profiles during a single discharge were obtained through the use of an optical multichannel analyzer (OMA), coupled to a one meter McPherson stigmatic monochromator. Using this apparatus, wavelength intervals covering approximately 15Å were recorded. Instrumental resolution was sufficient to yield calibration profiles with FWHM of less than .25Å. The time resolution of wavelength resolved measurements with the above equipment was adjustable but limited by the OMA's sensitivity and the light available to time periods greater than 5μsec. Due to this limited time resolution, and since only one gating interval could be accumulated during a discharge, another 1/2 meter spectrometer was used in conjunction with a photomultiplier to provide a continuous record of the light intensity in a given spectral bandpass throughout the time of the discharge.

A typical set of data collected by the OMA is shown in Figure 5. A 20μsec gating period beginning at the triggering of the discharge was used, so that this figure represents a time averaged spectra for that time interval. The most prominent feature in Figure 15 is the 4156.11Å ArII line with a smaller peak corresponding to the 4158.59Å ArI line also being readily apparent. Most

of the remaining features are instrumental noise except for the small peak immediately to the right of the ArII line and the series of peaks to the right of the ArI line. These peaks were found to reoccur on all similar data collected and correspond to OII and Al II impurities respectively. Using the ratios of integrated intensities for the above ArII and ArI lines in the Saha-Boltzmann ionization equilibrium relation, an average electron temperature of 1.4 eV was estimated.

Electron densities were determined from hydrogen line broadening after the introduction of a small percentage of H_2 in the primary argon gas. A typical H_γ profile is illustrated in Figure 6. Such data was reflected about the symmetry axis and then plotted on a log-log axis for comparison to the tabulated profiles of Vidal, Cooper and Smith.[8] A best fit of the H_γ profile of Figure 6 yielded an electron density near $2 \times 10^{14} cm^{-3}$. When considering this number it should be kept in mind that this is an average value integrated over both time (the gating was 15μsec in length beginning 5μsec after the discharge was triggered) and space (the light collection volume necessarily contained a large region around the gas nozzles), so that peak densities in the immediate vicinity of the gas nozzle may have been considerably higher.

Summary

In summary of these results, we report an apparatus which forms a hollow plasma shell of 3 cm x 2 cm cross section, 40 cm in diameter. This is done by first injecting a neutral gas shell of argon via 36 evenly spaced supersonic injection nozzles cut into two electrode plates. Nozzle system design

is such that the radial profile of the gas is sharply defined. Nozzle geometry gives Mach 6 injection which maintains a typical gas shell mass of a few hundred micrograms between the electrodes during quasi-steady injection. Noticeable azimuthal density modulation results from the highly confined injection pattern of each jet.

Electron temperatures of 1.4 eV and electron densities of $2\text{-}8 \times 10^{14} cm^{-3}$ are measured by spectroscopic techniques. Langmuir probe mapping of electron density indicates a discharge localized at each jet which is sensitive to details of the jet geometry. No strong diffusion perpendicular to the current flow is found. Open shutter photos of the discharge show luminosity patterns consistent with noticeable azimuthal modulation of the discharge.

Neutral gas density in the main flow is about $3 \times 10^{15} cm^{-3}$ which gives an ionization level of 10-50%. Langmuir probe profiles suggest that most of the current is carried by the low neutral density region created by the jet outwash. This current distribution is strongly confined by $\vec{J} \times \vec{B}$ forces giving little diffusion perpendicular to the current direction. We observed no indications of an implosion of the 36 current channels as would occur with a higher current.

Acknowledgements

This work was supported by AFOSR Grant 77-3259.

References

1. P.J. Turchi and W.L. Baker, J. Appl. Phys. 44, 4936 (1973).

2. W.L. Baker, M.C. Clark, J.H. Degnan, G.F. Kiuttu, C.R. McClenahan, R.E. Reinovsky, J. Appl. Phys. 49, 4694 (1978).

3. E.J.T. Burns, J.H. Degnan, R.E. Reinovsky, W.L. Baker, M.C. Clark, and C.R. McClenahan, Appl. Phys. Lett. 31, 477 (1977).

4. J. Shiloh, A. Fisher and N. Rostoker, Phys. Rev. Lett.. 40, 515 (1978).

5. C. Stallings, K. Childers, I. Roth, and R. Schneider, Appl. Phys. Lett. 35, 524 (1979).

6. I. Henins and J. Marshall, Rev. Sci. Instrum. 40, 875 (1969).

7. J.H. Degnan and R.E. Reinovsky, AFWL-TR-75-265 (1976).

8. C.R. Vidal, J. Cooper and E.W. Smith, Astrophys. J. Suppl. 25, 37 (1973).

FIGURE CAPTIONS

Figure 1. Drawing of gas shell injection geometry.

Figure 2. Drawing of supersonic injection nozzles and their orientation.

Figure 3. Typical discharge monitors: dI/dT(10 KA/Div) and gap voltage (2 KV/Div) open shutter photo as azimuthal homogeneity monitor.

Figure 4. Normalized electron density profile as a function of radial distance from center of jet. Curves are for t = 2μsec and 10 μsec after initiation of discharge.

Figure 5. Argon lines from OMA for determination of electron temperature.

Figure 6. H_β line profile used for determination of averaged electron density.

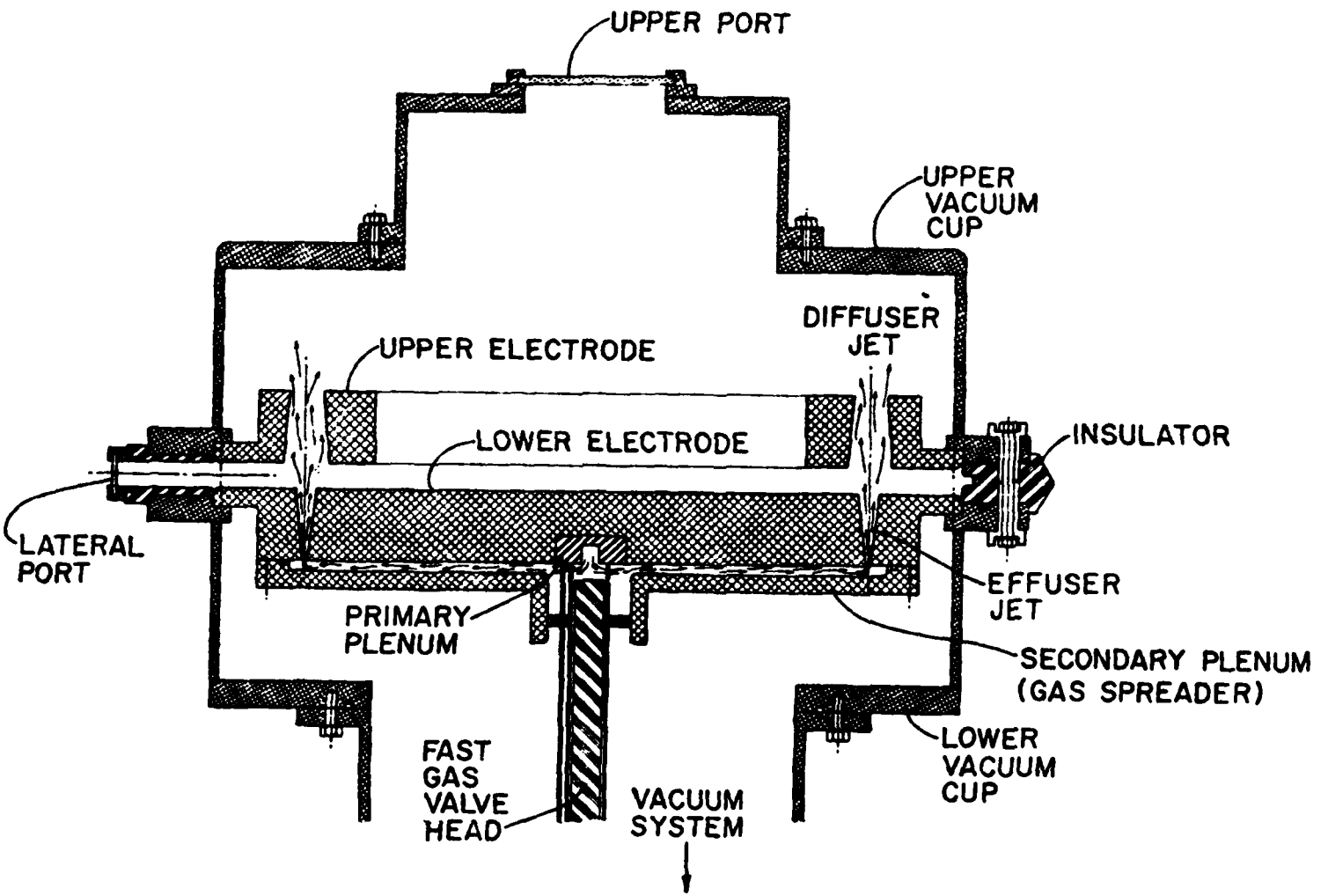
UPPER PORT
UPPER VACUUM CUP
DIFFUSER JET
UPPER ELECTRODE
LOWER ELECTRODE
INSULATOR
LATERAL PORT
EFFUSER JET
PRIMARY PLENUM
SECONDARY PLENUM (GAS SPREADER)
LOWER VACUUM CUP
FAST GAS VALVE HEAD
VACUUM SYSTEM

Figure 1.

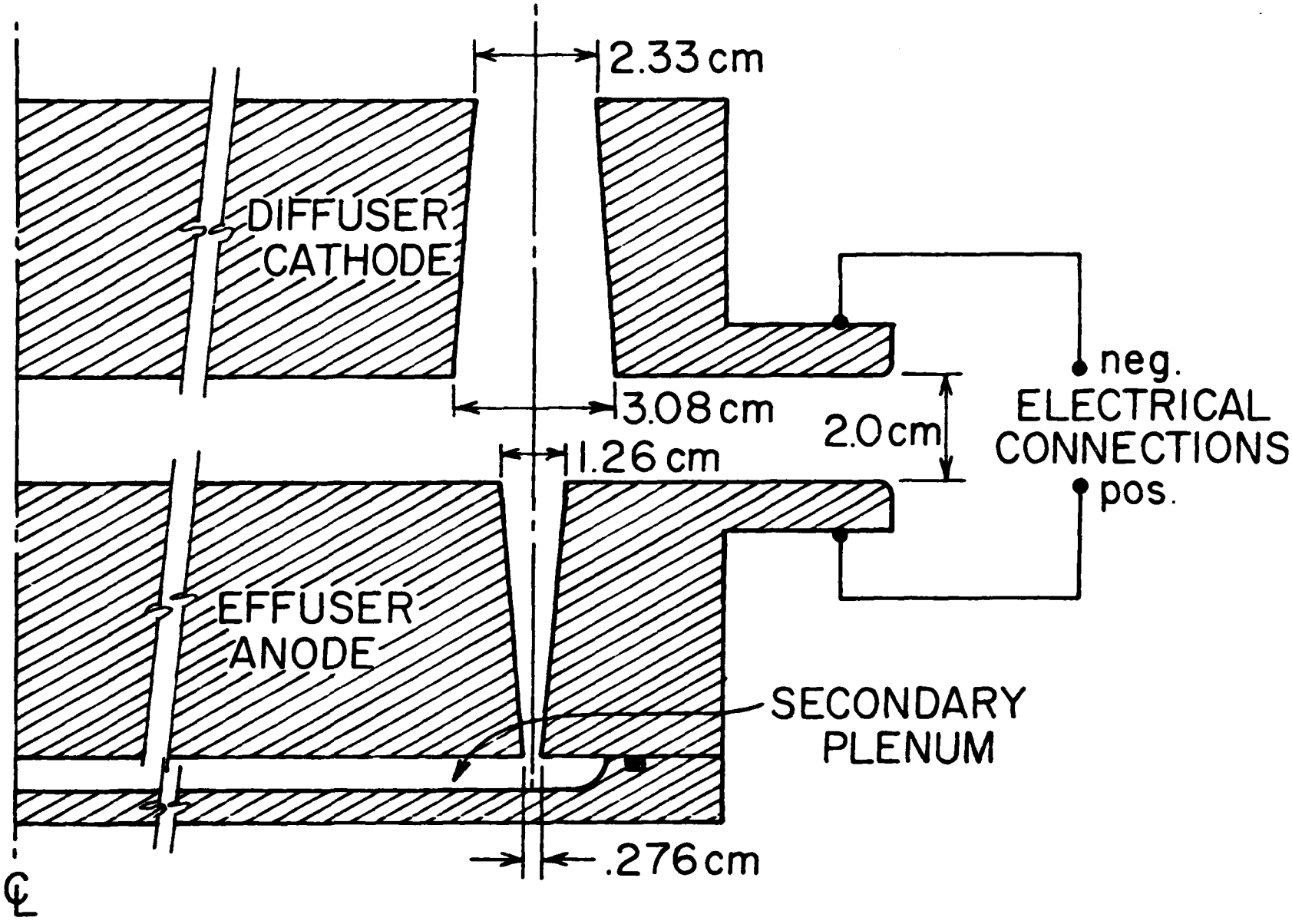

SUPERSONIC FLOW THRU NOZZLE GEOMETRY

Figure 2.

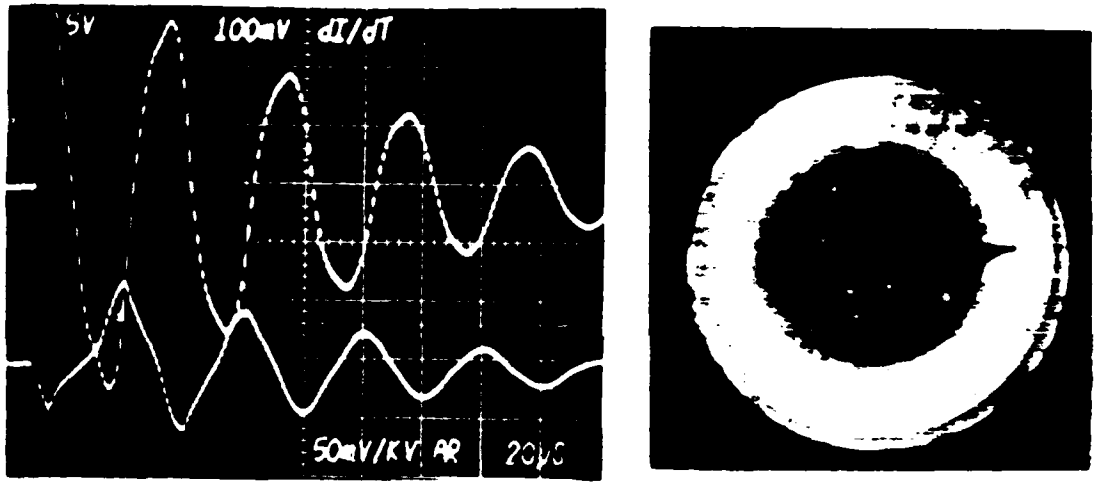

Figure 3.

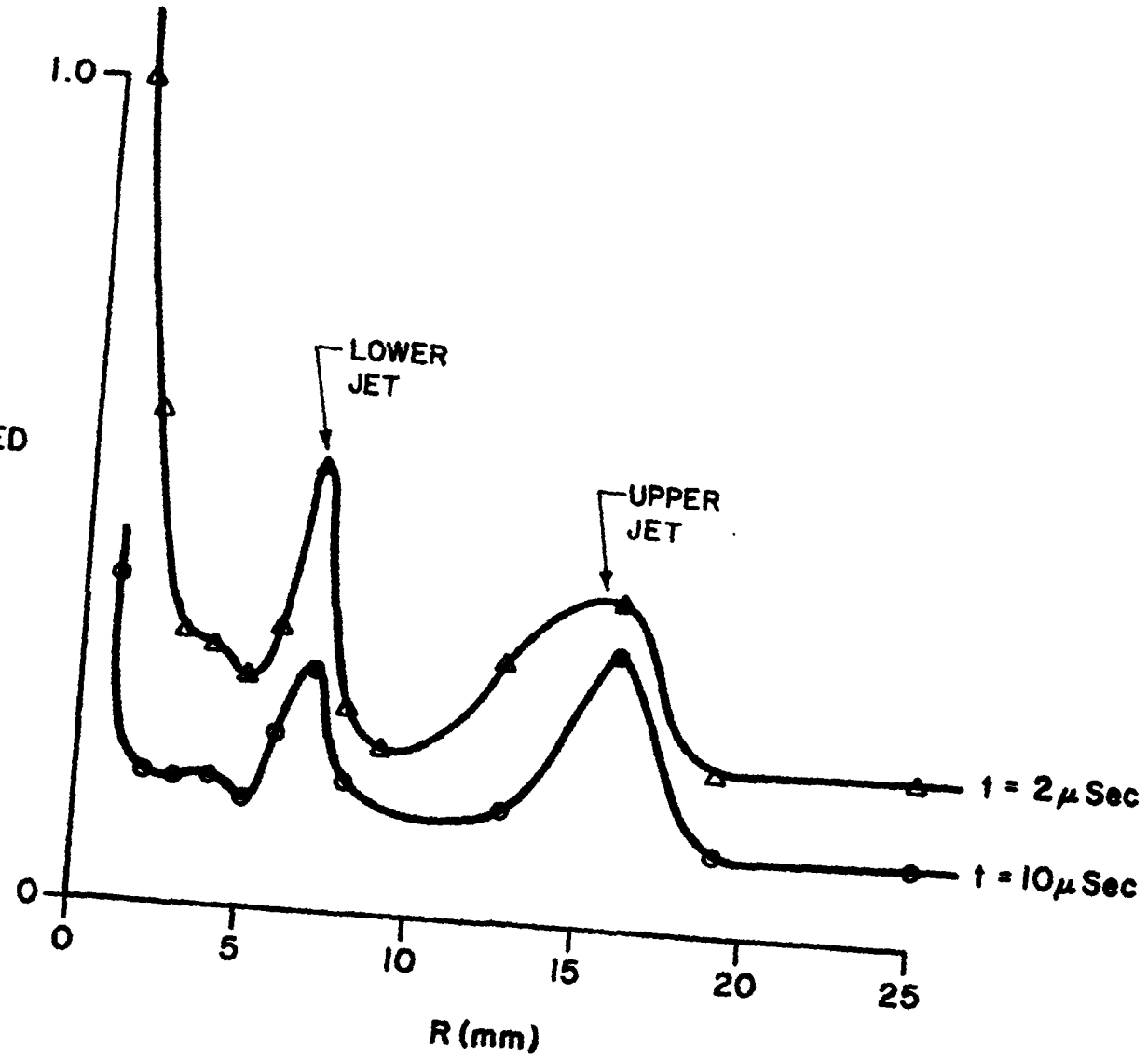
1.0
NORMALIZED
ELECTRON
DENSITY
LOWER
JET
UPPER
JET
t = 2μ Sec
t = 10μ Sec
0
0
5
10
15
20
25
R (mm)

Figure 4.

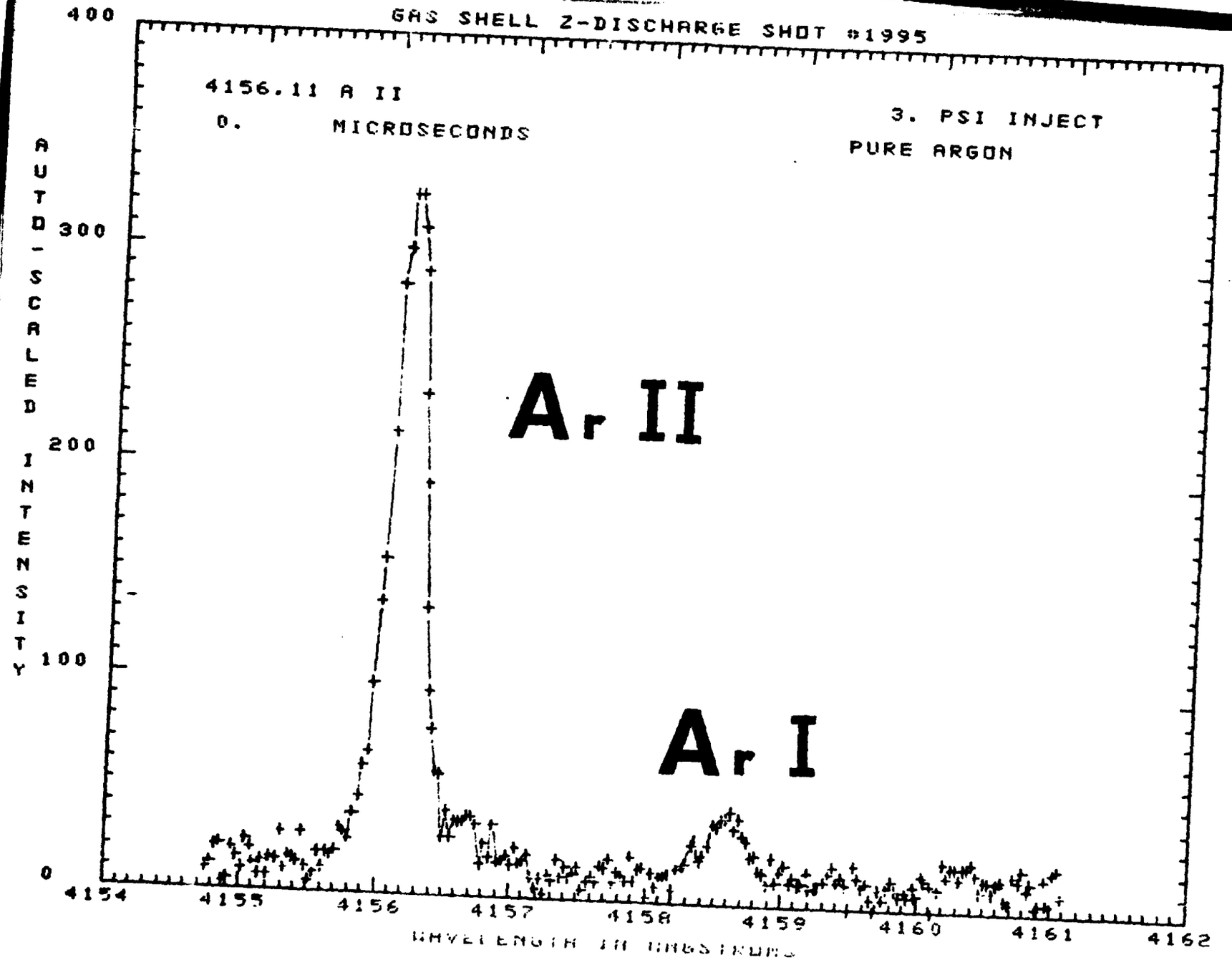
GAS SHELL Z-DISCHARGE SHOT #1995
4156.11 A II
0. MICROSECONDS
3. PSI INJECT
PURE ARGON
AUTO-SCALED INTENSITY
400
300
200
100
0
Ar II
Ar I
4154
4155
4156
4157
4158
4159
4160
4161
4162

Figure 5.

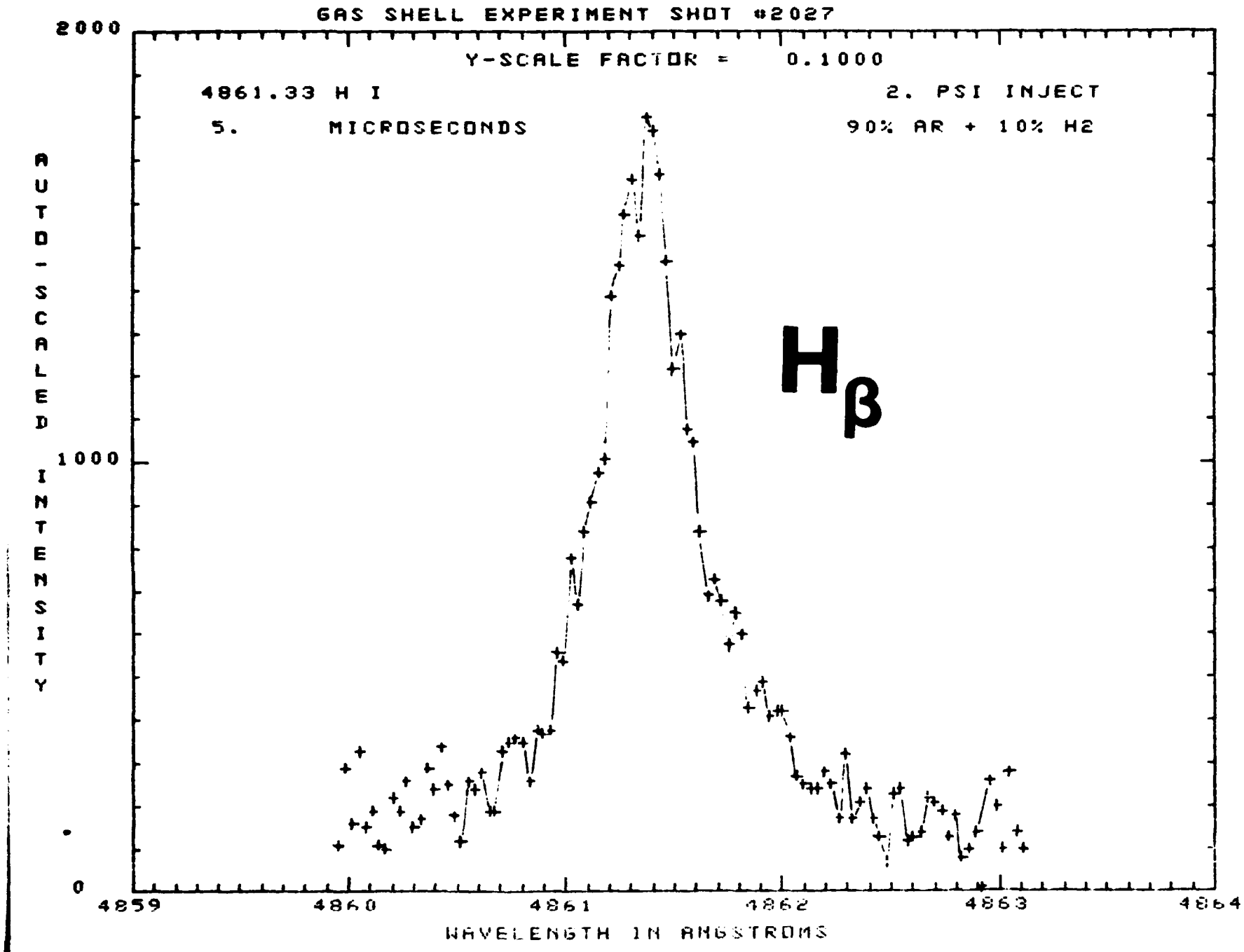
GAS SHELL EXPERIMENT SHOT #2027
Y-SCALE FACTOR = 0.1000
4861.33 H I
2. PSI INJECT
5. MICROSECONDS
90% AR + 10% H2
Hβ
AUTO-SCALED INTENSITY
2000
1000
0
4859
4860
4861
4862
4863
4864
WAVELENGTH IN ANGSTROMS

Figure 6.

UNCLASSIFIED

SECURITY CLASSIFICATION OF THIS PAGE (When Data Entered)

REPORT DOCUMENTATION PAGE	READ INSTRUCTIONS BEFORE COMPLETING FORM
1. REPORT NUMBER: AFOSR-TR- 80-0172 ✓	2. GOVT ACCESSION NO. / 3. RECIPIENT'S CATALOG NUMBER
4. TITLE (and Subtitle): FORMATION AND DIAGNOSTICS OF A CYLINDRICAL SHELL PLASMA	5. TYPE OF REPORT & PERIOD COVERED: Final
	6. PERFORMING ORG. REPORT NUMBER
7. AUTHOR(s): Roger D Bengtson	8. CONTRACT OR GRANT NUMBER(s): AFOSR 77-3259 ✓
9. PERFORMING ORGANIZATION NAME AND ADDRESS: Department of Physics ✓ University of Texas Austin, TX 78712	10. PROGRAM ELEMENT, PROJECT, TASK AREA & WORK UNIT NUMBERS: 61102F 2301/A7
11. CONTROLLING OFFICE NAME AND ADDRESS: AFOSR/NP Bolling AFB, Bldg. #410 Wash DC 20332	12. REPORT DATE: 1980
	13. NUMBER OF PAGES: 21
14. MONITORING AGENCY NAME & ADDRESS(if different from Controlling Office)	15. SECURITY CLASS. (of this report): unclassified
	15a. DECLASSIFICATION/DOWNGRADING SCHEDULE

16. DISTRIBUTION STATEMENT (of this Report)

Approved for public release; distribution unlimited.

17. DISTRIBUTION STATEMENT (of the abstract entered in Block 20, if different from Report)

18. SUPPLEMENTARY NOTES

19. KEY WORDS (Continue on reverse side if necessary and identify by block number)

20. ABSTRACT (Continue on reverse side if necessary and identify by block number)

An apparatus was developed which forms a hollow cylindrical plasma shell of 3 x 2 cm(2) cross section 40 cm diameter by injecting a neutral gas shell of argon via supersonic injection nozzles and ionizing this shell with a high voltage electrical discharge.

DD FORM 1 JAN 73 1473 EDITION OF 1 NOV 65 IS OBSOLETE

UNCLASSIFIED

SECURITY CLASSIFICATION OF THIS PAGE (When Data Entered)